Exploring Fully Superconducting Air-Core Machine Topology for Off-Shore Wind Turbine Applications

Dongsu Lee[1], Thanatheepan Balachandran[1], Han-Wook Cho[2], and Kiruba Haran[1], *Fellow, IEEE*

[1]Department of Electrical and Computer Engineering, University of Illinois at Urbana-Champaign, Urbana, IL 61801 USA
[2]Department of Electrical, Electronics, and Communications Engineering Education, Chungnam National University, Daejeon 305-764, South Korea

This paper presents an electromagnetic (EM) analysis and feasibility design study of a 10 MW air-core fully superconducting (SC) generator for off-shore wind turbine applications. This machine topology uses MgB_2 SC wires in both armature and field windings to reduce the generator cost. To reduce the weight of the machine, stator iron core in the traditional SC machine design is replaced with shield coils to contain the flux inside the machine. This air-core design allows the air-gap flux density to be increased without saturation to achieve an increased power density in machine design. Further, eliminating the iron core also eliminates the core losses. This is an attractive feature for off-shore wind turbine applications where machine weight can be reduced with increased efficiency. Preliminary EM studies are performed on a 10 MW, 10 r/min fully SC air-core machine design and its associated ac losses are evaluated. Design specification of the machine is provided with the armature, field, and shield winding parameter details. Finite element (FE) analysis is used to evaluate the flux density and torque profile of the machine. To reduce the ac losses in the armature coils, magnetic flux density at the armature winding is set to be 2 T. The preliminary results show this fully SC air-core generators show better performance in ac losses compared to the similar fully SC MW wind turbine designs.

Index Terms— **Air-core, fully superconducting (SC) machine, MgB_2, off-shore wind turbine, shield coils.**

I. Introduction

SUPERCONDUCTING (SC) electric machines hold immense promise for increased power density in electrical machines. They have been proposed and demonstrated for several high-power density applications, such as wind turbines, electric aircraft, and ship propulsion. Most of these applications have been developed using partially SC machines, which consist of conventional armature coils, made of copper or aluminum, and SC field coils. A fully SC machine topology uses superconductors in both armature and field coils. The topology can further improve the power density of SC machines. However, ac losses in the fully SC armature coils are difficult to manage and pose a significant barrier for the industrial application of these machines. Reducing the ac losses is very challenging, especially in relatively high-frequency machines such as those used in electric aircraft propulsion. However, wind turbines are an attractive application for fully SC machines because of their low frequency.

Another challenge of the SC machines is the core losses due to the high magnetic fields generated by the SC field coils. An air-core SC machine with SC shield coils has been proposed to eliminate these core losses [1]. In this machine topology, a shield coil is introduced radially apart from the field coil to cancel out the magnetic flux outside the machine. This design improves the specific power of the machine by eliminating core losses, the weight of the core, and minimized copper losses. In addition, it can obtain high efficiency above 99% even after considering the cryogenic cooling power. This approach was explored under a National Aeronautics and Space Administration (NASA) LEARN program, showing significantly improved power density in aerospace applications.

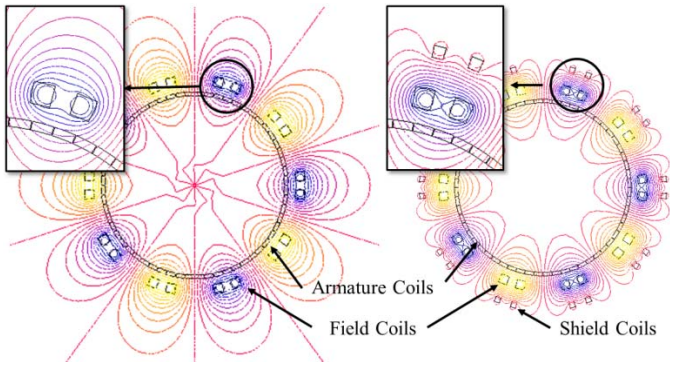

Fig. 1. Comparison of magnetic flux lines between shield and no shield.

Fig. 1 illustrates the shielding effects proposed in the active shield air-core SC machines. As shown in the figure, active shield coils retain the flux within the machine volume without using the iron yoke. This makes it practical to consider low-pole-count designs without increasing the weight. The low pole count helps reduce the ac losses in the SC armature coils. Fig. 2 shows the architecture of both machines with the iron yoke and with the shield coil. In this paper, the application of this machine topology is analyzed for use in 10 MW direct-drive off-shore wind turbine. The following effects of strength and location of the shield coils on various machine performance parameters will be explored in terms of torque production, superconductor usage, external flux, and ac copper

Manuscript received November 5, 2018; revised January 3, 2019; accepted March 6, 2019. Date of publication April 11, 2019; date of current version June 20, 2019. Corresponding author: K. Haran (e-mail: kharan@illinois.edu).

Color versions of one or more of the figures in this paper are available online at http://ieeexplore.ieee.org.

Digital Object Identifier 10.1109/TMAG.2019.2905591

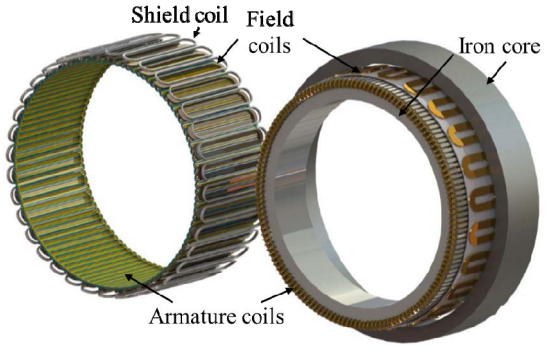

Fig. 2. Air-core architecture with shielding coils [air-core SC machine (left), iron core SC machine (right)].

loss. Methods to calculate ac losses, external flux, and cost are presented based on the finite element analysis (FEA).

Section II describes a fully SC generator design. Section III presents information on winding material, while Section IV shows ac loss characteristics and equations. Section V gives results based on the FEA and Section VI presents the conclusion.

II. Fully Superconducting Wind Generator

A. Machine Design

Fully SC machines for wind turbine applications have gained interest among researchers [2]–[10]. A 10 MW, 10 r/min fully SC machine using MgB_2 SC wires for both stator and rotor windings is proposed in [2]. In this machine topology, an iron core is deployed in both stator and rotor to reduce the usage of SC wire. A notable feature is a 10 mm copper electromagnetic (EM) shield installed on the outside surface of the rotor cryostat to intercept high-frequency harmonic fields created by the armature winding.

A feasibility study of a 10 MW, 4–11 r/min MgB_2 fully SC machine for an off-shore wind turbine including evaluation of SC ac losses is performed in [3]. Both armature and stator coils are employed using MgB_2 multifilament SC wires with a stator iron yoke. Flux density at the armature winding is limited to 2 T to reduce the ac losses. Total heat losses are estimated to be 2.2 KW, while the machine shows good electrical performances, and removing such a high heat load is not technically feasible. It is suggested that a low-pole machine could be more advantaged for a fully SC design. EM study of a 13.2 MW, 9 rpm fully SC machine with MgB_2 armature windings and low-temperature NbTi SC, and a stator iron yoke is studied in [4]. Race-track coils are adapted for field windings. Here, the design flux density at the armature winding is set to be 2.5 T. Ac losses are estimated to be 2.93 kW. A 15 MW, 10 rpm fully SC machine using rare-earth barium copper oxide SC tapes and a back-iron yoke is proposed in [5]. A notable feature of this machine is the operating temperature set at 40 K. The flux density at the air gap is set to be 2 T. Ac losses in the armature winding are estimated to be around 4 kW.

A 10 MW, 10 rpm wind turbine generator with MgB_2 armature windings and high temperature superconductor SC yttrium barium copper oxide tapes for field windings with a back-iron core is proposed in [6]. Three different machine designs are considered and compared to their performance and ac losses. Minimum ac losses at no-load condition across all these designs were 1.06 kW at the maximum allowable flux density when the armature coils are set at 3 T. Another 10 MW, 10 r/min machine with the aforementioned winding topology is studied in [7]. In this design, the maximum flux density observed at the armature winding is 3.42 T and the corresponding ac losses are kept under 1 kW. It is shown that this fully SC machine design can reduce 16% of the weight of the equally rated partially SC machine. All these topologies employed iron core, including high core loss due to saturation and weight.

Decreasing SC material cost and manufacturability of longer wires enables designs using more SC material [1]. However, a tradeoff between the cost of SC conductors and the performance of the machine design for specified application needs to be considered. The key design is eliminating the iron core, which pushes the air-gap flux density to a higher value to achieve higher power density machines. A 10 MW, 3000 r/min electric machine is proposed for electric propulsion in this paper. The design shows 17% more SC material compared to the same specifications of the back-iron machine topology. An optimal design is studied in [8]. Results show that the machine volume can be reduced with compensation of more SC usage. In this design, the armature coil flux density is set to be 2 T. Effects of pole count are studied in [9]. Results show that lower pole-count designs allow a reduction in the volume and heat losses. An analytical evaluation of ac losses for different air-core machine designs is presented [10]. Fully and partial air-core SC machine topologies are studied. Results show that a 10 MW, 10 r/min fully SC design without a stator iron core has ac losses estimated at 580 W. This is comparatively smaller than the similar 10 MW wind turbine generator designs proposed in the literature. However, this paper does not include EM, torque profile, or feasibility study of the machine.

High power density features are very attractive for wind turbine applications. A 10 MW, 10 r/min fully SC air-core machine for wind turbine generator application is considered in this paper. Detailed EM and feasibility studies of the design are performed. The torque profile and the ac losses are evaluated and compared with the similar 10 MW, 10 r/min machine.

B. Specifications

Specifications of the proposed 10 MW SC generator are summarized in Table I. The low-speed design (10 rpm) is the key challenge. Ac losses and efficiency are calculated and compared with other MW wind turbine designs.

Design of the targeted machine is shown in Fig. 3. As is explained in [1], the iron core is replaced with shield coils to contain the flux inside the machine. Each pair of shield coils is placed radially apart from each field coil. A 40-pole machine topology is considered with six armature slots per pole. Armature flux density and coil current densities are

TABLE I
SPECIFICATION OF FULLY SC GENERATOR

Design parameter	Value
Rated power [MW]	10
Speed [rpm]	10
Operating temperature [K]	20
No. of poles	40
Number of phase	3
Rated voltage [V_{rms}] / current [A_{rms}]	6,600 / 874
Air gap [mm]	40
Diameter [mm]	1,940
Axial length [mm]	535
Armature current density [A/mm^2]	140
Field and shield current density [A/mm^2]	200

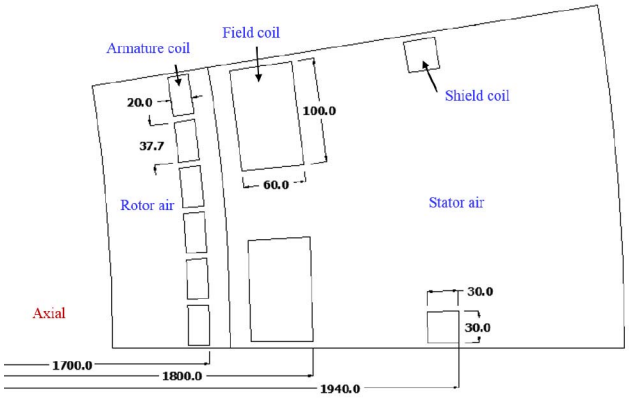

Fig. 3. Configuration of the SC generator (unit [millimeter]).

predefined to allow a safety margin from critical current values.

C. Superconducting Material

MgB_2 wires, similar to described in [11] were chosen as SC wires due to their low ac loss characteristics at the 20 K operating temperature. This is a multi-filamentary composite wire used in armatures, as well as field and shield windings. The main parameters of the chosen wire are tabulated in Table II. Hysteresis and coupling ac losses depend on these wire parameters and are used to evaluate these machine ac losses.

III. STATOR, ROTOR, AND SHIELD WINDINGS

The size of the MgB_2 composite wire and the measured critical current density at self-field is listed in Table II. Operating current of the selected MgB_2 wire is set to be 200 A/mm^2 at 20 K. This operating point is chosen below the critical current densities of the wires to allow for a margin of safety [10], [12]. Armature current density is set to 140 A/mm^2 because the higher value of currents tends to dominate and distort air gap B field distribution.

The maximum magnetic field calculated in the armature winding is set to be 2.0 T to lower the ac losses generated in the armature coils.

TABLE II
MAIN PARAMETERS OF MgB_2 WIRE

Symbol	Parameter	Value
B_m	- The peak-to-peak amplitude of the magnetic flux at ar mature winding (penetration field)	Max - 2.0T
J_c	Critical current density at self-field at 20K [A/m^2]	2.8e9
ω	- Angular speed [rad/s]	20.94
D_SC	- SC diameter [mm]	0.6
a	- Filament diameter [mm]	0.01
n	- Number of filament	360
λ	- The area fraction of the wire that is SC	10%
A	- The wire's internal eddy current shielding factor	0.7
β	- The ratio of the applied magnetic field to the intrinsic p enetration field (B_p) quantity of the SC filaments	B_m/B_p
Γ	- A dependent constant for hysteresis loss	-
P_e	- Effective transverse resistivity [Ω-m]	2.3e-8
L	- The twist pitch	0.005

IV. AC LOSS CHARACTERISTICS OF SC GENERATOR

Ac losses are calculated using the Wilson model described in [13]. Wilson developed a loss function $\Gamma(\beta)$ to capture the dependence of hysteresis loss on the applied field strength and simplified the hysteresis loss equation as follows:

$$Q_h = \frac{B_m^2}{2\mu_0}\Gamma(\beta) \tag{1}$$

where B_m is the peak-to-peak amplitude of magnetic flux at the armature winding (penetration field), μ_0 is the air permeability, and $\Gamma(\beta)$ is a function evaluated by integrating the magnetization energy in the hysteresis loop across various penetration states. Hysteresis loss due to the simultaneous field and current in an electric machine is studied in [14]. It is shown that ac losses in an application where the field will be large and the current relatively small can be evaluated as

$$Q_h = \frac{B_m^2}{2\mu_0}\Gamma(\beta)\frac{Q(H_0, I_0)}{Q(0, I_0)} \tag{2}$$

where $Q(H_0, I_0)/Q(0, I_0)$ is loss multiplication factor, and I_0 and H_0 are the amplitude of transport current and magnetization by transport current, respectively.

This model is adopted in [10] to calculate the ac losses in the armature windings. The ac loss calculation was evaluated based on work in [10]. Flux density in the armature winding is evaluated using the FE analysis. Ac losses consist of hysteresis loss can be evaluated as

$$Q_h = \frac{B_m^2\lambda}{2\mu_0(\omega^2\tau_a^2+1)}\Gamma\left(\frac{\beta}{(\omega^2\tau_a^2+1)^{\frac{1}{2}}}\right)\frac{Q(H_0, I_0)}{Q(0, I_0)} \tag{3}$$

where λ is the superconductor filling factor of the wire, τ is the LR time constant of the wire cross section, a is the wire's internal eddy current shielding factor, and ω is an angular speed, as listed in Table II. Eddy current losses or coupling losses can be evaluated as

$$Q_c = \frac{B_m^2}{2\mu_0}\frac{\alpha\pi\omega\tau_a}{(\omega^2\tau_a^2+1)} \tag{4}$$

where $\tau = (\mu_0/2\rho_t)(L/2\pi)^2$, $B_p = 4^*\mu_0^* J_c^* a/\pi$, $\tau_\alpha = \tau\alpha$.

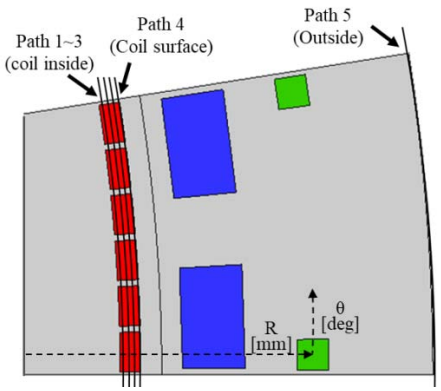

Fig. 4. Paths and shield coil paths used to analyze the flux density.

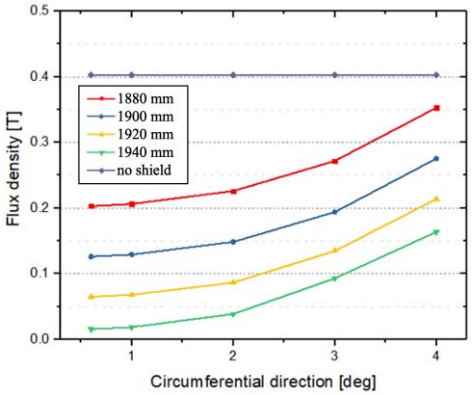

Fig. 5. Flux density (path-5) according to the shield coil location.

Penetration loss is calculated as

$$Q_p = \frac{B_m^2 \omega^2 \tau_\alpha^2}{2\mu_0(\omega^2\tau_\alpha^2+1)}\Gamma\left(\frac{\beta\omega\tau_\alpha}{(\omega^2\tau_\alpha^2+1)(n\lambda)^{\frac{1}{2}}}\right) \quad (5)$$

where n is the number of filaments.

Total machines ac losses are evaluated as follows:

$$P_t = (Q_c + Q_p + Q_h)V_a f \quad (6)$$

where V_a is the armature winding volume and f is the frequency. The Q_c, Q_p, and Q_h are average hysteresis, coupling, and eddy current losses calculated across a single SC wire per cycle per cubic meter. Multiplying by the wire cross-sectional area, and frequency f will result in loss in watts per meter. Finally, the result is multiplied by the conductor length to find the total ac loss in the armature

V. Numerical Analysis Based on FEA

This section presents numerical EM results for the 10 MW SC generator in terms of torque production, ac loss, and flux density. In addition, the location of the shield coils is changed and the impact of the location of the shield coils in the flux density and torque production is also analyzed. Since the magnitude of ac loss is dependent on the maximum flux density experienced by the armature coils, the flux density at the armature coils is evaluated in several paths around the coils as shown in Fig. 4. To limit the ac losses in the armature coil, path-4 located at the armature surface set to have the maximum flux density of 2.00 T.

The flux density outside the shield coils was also analyzed to identify the best location of the shield coils which minimizes the outside field values. To analyze the field values outside the shield coils, path-5 is set at 140 mm radially outward from the field coils and the flux density is measured. Twenty different machine designs are considered by changing the shield coils location along the radial direction R and circumferential direction θ as shown in Fig. 4.

Fig. 5 shows magnetic flux density variation measured at path-5 according to the shield coil locations in the no-load condition. These results are compared with the no-shield machine design flux density value of 0.402 T. As shown in Fig. 5, when the shield coils are placed radially further apart from the field coils, outside flux density decreases with the radial distance. However, this results in an increase in the

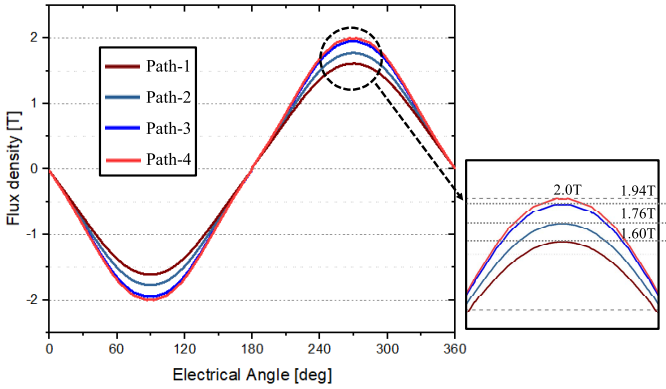

Fig. 6. Flux density distribution according to Paths 1–4.

TABLE III
AC Loss Results

Classification		Hysteresis	Eddy current	Penetration
Flux density	Path-1	1.60 T		
	Path-2	1.76 T		
	Path-3	1.94 T		
Ac loss	Path-1	128 [W]	100 [W]	0 [W]
	Path-2	141 [W]	121 [W]	0 [W]
	Path-3	155 [W]	147 [W]	0 [W]
	Sum	424 [W]	368 [W]	0 [W]
Total ac loss [W]		792 [W]		

diameter of the machine. Since the maximum diameter of the machine is set to be 2000 mm, the best model is chosen when the shield coils are located at 1940 mm. When the circumferential direction between the shield coils is decreased, outside flux density increased. A model with lowest flux density (0.02 T) is selected as the best model with the shield coil located radially at 1940 mm and 0.6° which corresponds to 7.8° between two shield coils.

To obtain B_m in (1), the flux density waveforms were evaluated at paths 1–4, as shown in Fig. 6. As shown in Fig. 6, the maximum flux density is decreased as the conductors are located further away from the field coils. Therefore, to include this effect on the ac loss calculation, ac losses are evaluated assuming a uniform flux density which is equal to the maximum flux density of each path region and the average ac losses are calculated. Hysteresis, eddy current, and

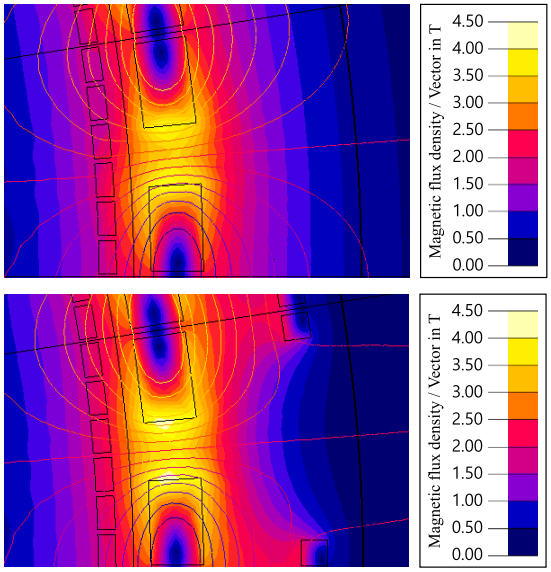

Fig. 7. Flux density distribution according to the shield coil [No-shield coil design (top), Shield coil design (bottom)].

TABLE IV
RESULTS OF MAIN PARAMETERS

Classification	Parameter	Value
Common	Superconductor	MgB_2
	Slot fill factor	0.5
	Number of SC per cable	7
	Expected cost of cable	3$/m
	Operating temperature	20K
Armature winding	Inner radius [mm]	1,680
	Outer radius [mm]	1,700
	Current density [A/mm^2]	140
	Mean length per cable turn [m]	1.50
	Cable turns per slot (240 slots)	190
	Total SC cable usage [km]	34.2
	Cost [k$]	102.6
Field winding	Inner radius [mm]	1,740
	Outer radius [mm]	1,800
	Current density [A/mm^2]	200
	Mean length per cable turn [m]	1.39
	Cable turns per slot (80 slots)	1516
	Total SC cable usage [km]	84.3
	Cost [k$]	252.9
Shield winding	Inner radius [mm]	1,910
	Outer radius [mm]	1,940
	Current density [A/mm^2]	200
	Mean length per cable turn [m]	1.48
	Cable turns per slot (80 slots)	227
	Total SC cable usage [km]	13.4
	Cost [k$]	40.3

penetration losses are evaluated in a similar manner and the average total ac losses are tabulated in Table III. As a result, the hysteresis loss (424 W) is higher than the eddy current loss (368 W), while the penetration loss is almost 0.

Fig. 7 shows the flux density of the generator compared with no-shield generator. As shown in the figure, when the shield coils are introduced, the outside field values are reduced. The best model shows 95% of field reduction in the outside field values at path-5. However, the shield coils negatively impact the flux density in the armature coils. When the field coils are introduced, the flux density at the armature coils is reduced by 3.5%. As a result, the torque of the shield coil design is slightly reduced from 10.01 to 9.65 MN · m.

Proposed machine design parameters, total SC usage, and SC cost are tabulated in Table IV. The cost of MgB_2 cable (7 strands) is assumed to be 3$/m. As a result, the total cost of MgB_2 is estimated to be 396 k$. This is higher than the total SC cost reported on references [3], [15], but it is expected since the machine has higher efficiency and lower weight.

VI. CONCLUSION

A 10 MW, 10 r/min fully SC air-core machine design is proposed for off-shore wind turbines application. The proposed generator topology aims to reduce machine weight, cost, and ac losses. To achieve these aggressive goals, the SC generator was designed as a fully SC machine employing MgB_2 wires in armature and field coils. To reduce the weight and increase the power density, the iron core is eliminated and replaced with shield coils to contain the flux inside the machine. The performances of the generator were analyzed based on the FEA in terms of torque production, ac loss, and impact of the shield coil. Preliminary results show that the shield coil reduces outside flux by 95% compared to no-shield design. However, shield coil design torque production is slightly decreased by 3.5% compared with the no-shield design. The ac loss of the machine is evaluated as 792 W; this is a low value compared to the other MW fully SC designs. However, further analysis needs to be conducted to validate this estimated ac loss. Low ac losses are achieved through the limited flux density of 2 T around armature coils and comparatively small air-gap (40 mm) design. The proposed machine design is not optimized for the performance and minimum SC usage. An optimal design of the machine will be presented in future works. Mechanical assembly of this motor will be similar to [2] where both rotor and stator assemblies are mechanically and thermally independent. This design provides the most flexibility for ease of operation and service. Furthermore, an inside-out synchronous machine design topology will be adopted, where dc excitation poles will be on the outside rotor and ac armature winding on the inside stator. A king-pin nacelle design by mounting the generator in front of the turbine similar to [3] also will be investigated. A detailed mechanical design of the proposed machine topology will be presented in future works.

ACKNOWLEDGMENT

This work was supported by the United States National Science Foundation under Grant 1807823.

REFERENCES

[1] K. S. Haran, D. Loder, T. O. Deppen, and L. Zheng, "Actively shielded high-field air-core superconducting machines," *IEEE Trans. Appl. Supercond.*, vol. 26, no. 2, Mar. 2016, Art. no. 5202508.

[2] S. S. Kalsi, "Superconducting wind turbine generator employing MgB_2 windings both on rotor and stator," *IEEE Trans. Appl. Supercond.*, vol. 24, no. 1, Feb. 2014, Art. no. 5201907.

[3] A. B. Abrahamsen, N. Magnusson, D. Liu, E. Stehouwer, B. Hendriks, and H. Polinder, "Design study of a 10 MW MgB_2 superconductor direct drive wind turbine generator," in *Proc. Eur. Wind Energy Assoc. (EWEA)*, 2014, pp. 1-7.

[4] F. Lin, R. Qu, D. Li, Y. Cheng, and J. Sun, "Electromagnetic design of 13.2 MW fully superconducting machine," *IEEE Trans. Appl. Supercond.*, vol. 28, no. 3, Apr. 2018, Art. no. 5205905.

[5] M. Saruwatari *et al.*, "Design study of 15-MW fully superconducting generators for offshore wind turbine," *IEEE Trans. Appl. Supercond.*, vol. 26, no. 4, Jun. 2016, Art. no. 5206805.

[6] Y. Terao, M. Sekino, and H. Ohsaki, "Electromagnetic design of 10 MW class fully superconducting wind turbine generators," *IEEE Trans. Appl. Supercond.*, vol. 22, no. 3, Jun. 2012, Art. no. 5201904.

[7] Y. Liang, M. D. Rotaru, and J. K. Sykulski, "Electromagnetic simulations of a fully superconducting 10-MW-class wind turbine generator," *IEEE Trans. Appl. Supercond.*, vol. 23, no. 6, Dec. 2013, Art. no. 5202805.

[8] D. C. Loder and K. S. Haran, "Multi-objective optimization of an actively shielded superconducting field winding," in *Proc. IEEE Power Energy Conf. Illinois (PECI)*, Feb. 2015, pp. 1–4.

[9] D. C. Loder and K. S. Haran, "Multi-objective optimization of an actively shielded superconducting field winding: Pole count study," in *Proc. IEEE Int. Electr. Mach. Drives Conf. (IEMDC)*, May 2015, pp. 1709–1714.

[10] M. Feddersen, K. S. Haran, and F. Berg, "AC loss analysis of MgB_2-based fully superconducting machines," *IOP Conf., Mater. Sci. Eng.*, vol. 279, no. 1, Dec. 2017, Art. no. 012026.

[11] F. Wan, M. D. Sumption, M. A. Rindfleisch, M. J. Tomsic, and E. W. Collings, "Architecture and transport properties of multifilamentary MgB_2 strands for MRI and low AC loss applications," *IEEE Trans. Appl. Supercond.*, vol. 27, no. 4, Jun. 2017, Art. no. 6200105.

[12] G. Li *et al.*, "Transport critical current densities and n-values of multifilamentary MgB_2 wires at various temperatures and magnetic fields," *IEEE Trans. Appl. Supercond.*, vol. 24, no. 3, Jun. 2014, Art. no. 6200105.

[13] M. N. Wilson, *Superconducting Magnets*. Oxford, U.K.: Clarendon, 1983.

[14] J. J. Rabbers, D. C. V. D. Laan, B. T. Haken, and H. H. J. T. Kate, "Magnetisation and transport current loss of a BSCCO/Ag tape in an external AC magnetic field carrying an AC transport current," *IEEE Trans. Appl. Supercond.*, vol. 9, no. 2, pp. 1185–1188, Jun. 1999.

[15] A. B. Abrahamsen *et al.*, "Comparison of levelized cost of energy of superconducting direct drive generators for a 10-MW offshore wind turbine," *IEEE Trans. Appl. Supercond.*, vol. 28, no. 4, Jun. 2018, Art. no. 5208205.